

Mössbauer Spectroscopy Evidence for Phase Selectivity in Excimer Laser Induced Amorphization of Thermally Annealed FeCoBSi Metallic Glass *

M. Sorescu^a and E. T. Knobbe^b

^a Oklahoma State University, Department of Chemistry, Stillwater, Oklahoma 74078-0447 and Duquesne University, Bayer School of Natural and Environmental Sciences, Mellon Hall, Pittsburgh, Pennsylvania 15282-1503, USA **

^b Oklahoma State University, Department of Chemistry and Noble Center for Laser Research, Stillwater, Oklahoma 74078-0447, USA

Z. Naturforsch. **51a**, 389–395 (1996); received February 3, 1996

Pulsed excimer laser irradiation effects ($\lambda = 308$ nm, $\tau = 10$ ns, $w = 3$ J/cm², $N = 2$ laser pulses/spot, repetition rate 1 Hz) on the magnetic properties and phase composition of thermally annealed Fe₆₆Co₁₈B₁₅Si₁ metallic glass have been studied by transmission and conversion electron Mössbauer spectroscopy (CEMS). Radiation-driven surface modifications were examined by scanning electron microscopy (SEM). Excimer laser induced amorphization was observed in partially crystallized Fe₆₆Co₁₈B₁₅Si₁ samples ($T_A = 648$ K, $t_A = 1$ hour) and was found to be accompanied by the development of laser-induced magnetic anisotropy. In totally crystallized Fe₆₆Co₁₈B₁₅Si₁ specimens ($T_A = 723$ K, $t_A = 1$ hour), the effect of excimer laser induced amorphization exhibited phase selectivity with respect to the crystalline components of the alloy system. When compared to bulk data, a different behavior of the surface magnetic texture and relative abundance of alloy phases was observed. The laser-induced phase transformation of thermally annealed Fe₆₆Co₁₈B₁₅Si₁ specimens was shown to consist of partial amorphization and surface oxidation of the irradiated material.

Key words: Metallic glasses, Laser processing, Phase transformations, Magnetic properties, Mössbauer spectroscopy

Introduction

In order to understand and modulate the fundamental properties of advanced magnetic materials, a promising approach is to establish and correlate the mechanisms and controlling factors of microstructure, magnetic texture, and selective phase transformations in amorphous systems during laser processing.

Recently, we proposed the use of pulsed excimer laser radiation to study unconventional aspects of materials response by selectively inducing localized changes in the system under investigation [1–7]. Fundamental effects underlying the interaction of excimer laser radiation with amorphous metals, such as excimer-laser-induced magnetic anisotropy [1, 3–5] and excimer-laser-induced crystallization [2, 5] were demonstrated and found to depend on the values of the irradiation parameters and materials properties.

The present study has been performed in order to explore the possibility of controlling the magnetic texture and phase equilibrium in thermally annealed Fe-Co based metallic glasses by means of excimer laser irradiation. Due to its local-probe character and the possibility of investigating both bulk and surface characteristics separately, Mössbauer spectroscopy was used to monitor the changes in magnetic anisotropy and phase composition, induced by employing different thermal annealing and laser irradiation treatments. Complementary information on related morphological changes was obtained using SEM. Excimer-laser-induced amorphization effects were demonstrated in partially and completely crystallized Fe₆₆Co₁₈B₁₅Si₁ samples and found to exhibit selectivity with regard to the crystalline phases in the alloy system.

Experimental

Amorphous alloy Fe₆₆Co₁₈B₁₅Si₁ (Metglas 2605 CO) was supplied by Allied Signal Inc. in the form of

* Presented at the XIIIth International Symposium on Nuclear Quadrupole Interactions, Providence, Rhode Island, USA, July 23–28, 1995.

** Permanent address after August 18, 1995; reprint requests to Prof. M. Sorescu.



20 μm thick ribbons. The material has a Curie temperature $T_C = 688$ K, a crystallization temperature $T_x = 703$ K, and a magnetostriction constant of 35 ppm.

Partially and completely crystallized $\text{Fe}_{66}\text{Co}_{18}\text{B}_{15}\text{Si}_1$ samples were prepared by annealing the amorphous specimens for $t_A = 1$ hour at $T_A = 648$ K and 723 K, respectively. These samples were further exposed to the $\lambda = 308$ nm radiation generated by a XeCl excimer laser (Lambda Physik), with the pulse width $\tau = 10$ ns, capable of giving an energy $W_p = 75$ mJ/pulse. A single-pulse energy density $w = 3$ J/cm², corresponding to a laser fluence $\Phi_L = 5 \times 10^{18}$ photons/cm² was achieved by focusing with a cylindrical fused-silica lens to a spot size of 0.5×5 mm². Thermally annealed samples of $\text{Fe}_{66}\text{Co}_{18}\text{B}_{15}\text{Si}_1$ were irradiated with 2 laser pulses per spot at a repetition rate of 1 Hz. An acceptable degree of homogeneity was obtained by laser-beam scanning of the sample surface, which was placed on an x-y-z micrometer translation stage.

Room-temperature transmission Mössbauer spectra were recorded with the γ -ray perpendicular to the ribbon plane using a constant acceleration spectrometer (Ranger Scientific). The 25 mCi γ -ray source was ^{57}Co diffused in Rh matrix, maintained at room temperature.

CEMS spectra of as-annealed and laser-treated surfaces of the metallic samples were collected using a flowing He-CH₄ electron counter [8]. The back-scattered electrons into 2π solid angle were recorded, so that the behavior of surface layers of ~ 100 nm could be detailed.

Least-squares fitting of the Mössbauer spectra corresponding to thermally annealed and laser irradiated samples was performed with the NORMOS DIST program [9] in the assumption of Lorentzian line-shapes. The program uses the constrained Hesse-Rübartsch method to extract the hyperfine field distributions and can analyze superpositions of field distributions and crystalline sites. The relative areas of the outer:inner line pairs of the amorphous component were constrained to the ratio 3:1.

SEM investigations were performed without further surface preparation using a JEOL electron microscope at 25 keV, operating in the secondary-electron-emission mode.

Results and Discussion

Figure 1a shows the room-temperature transmission Mössbauer spectrum of the $\text{Fe}_{66}\text{Co}_{18}\text{B}_{15}\text{Si}_1$ sample, after thermal annealing at 648 K for 1 hour. The sharp six-line pattern in the Mössbauer spectrum exhibits a hyperfine magnetic splitting of 362.1 kOe and corresponds to the α -(FeCo) crystalline phase. This result is in agreement with the previous identification of α -(FeCo) in the primary crystallization process of $\text{Fe}_{78-x}\text{Co}_x\text{Si}_9\text{B}_{13}$ amorphous alloy, based on differential thermal analysis [10].

For the 14.4 keV γ -rays of ^{57}Fe , the relative intensity of the second (fifth) to the first (sixth) lines is given, in the thin absorber approximation, by $R_{21} = 4 \sin^2 \alpha / [3(1 + \cos^2 \alpha)]$, where α is the angle between the γ -ray propagation direction and the direction of the net magnetic moment. The ratio R_{21} varies from 0 to 4/3 as α changes from 0° to 90° and for a completely random distribution of magnetic-moment directions, takes the value 0.67. Thus, the R_{21} values in Table 1 indicate that the magnetic moments of the α -(FeCo) crystalline phase are preferentially oriented in the plane of the foil. The hyperfine magnetic field distribution shown in Fig. 1A corresponds to the remaining amorphous matrix. The partially-crystallized sample was further exposed to pulsed-excimer-laser irradiation ($\Phi_L = 5 \times 10^{18}$ photons/cm²) with 2 laser pulses per spot at a repetition rate of 1 Hz. The room-temperature transmission Mössbauer spectrum and hyperfine magnetic field distribution of the irradiated $\text{Fe}_{66}\text{Co}_{18}\text{B}_{15}\text{Si}_1$ sample are shown in Figs. 1b and 1B, respectively. It can be inferred from Table 1 that the α -(FeCo) content decreased from 11.5% in the thermally-annealed system to 7.1% in the laser-exposed specimen. At the same time, a pronounced out-of-plane reorientation of the magnetic-moment directions resulted as an effect of the laser irradiation performed. Consequently, excimer-laser-induced reorientation was evidenced in the partially-crystallized $\text{Fe}_{66}\text{Co}_{18}\text{B}_{15}\text{Si}_1$ system and was found to be accompanied by the development of laser-induced magnetic anisotropy.

In order to obtain a complete characterization of the laser-induced phase transformation in $\text{Fe}_{66}\text{Co}_{18}\text{B}_{15}\text{Si}_1$ glassy ferromagnet, a separate surface analysis of the partially-crystallized and laser-irradiated specimens has been performed. Figures 1c and 1d show the conversion electron Mössbauer spectra of the $\text{Fe}_{66}\text{Co}_{18}\text{B}_{15}\text{Si}_1$ samples, after thermal an-

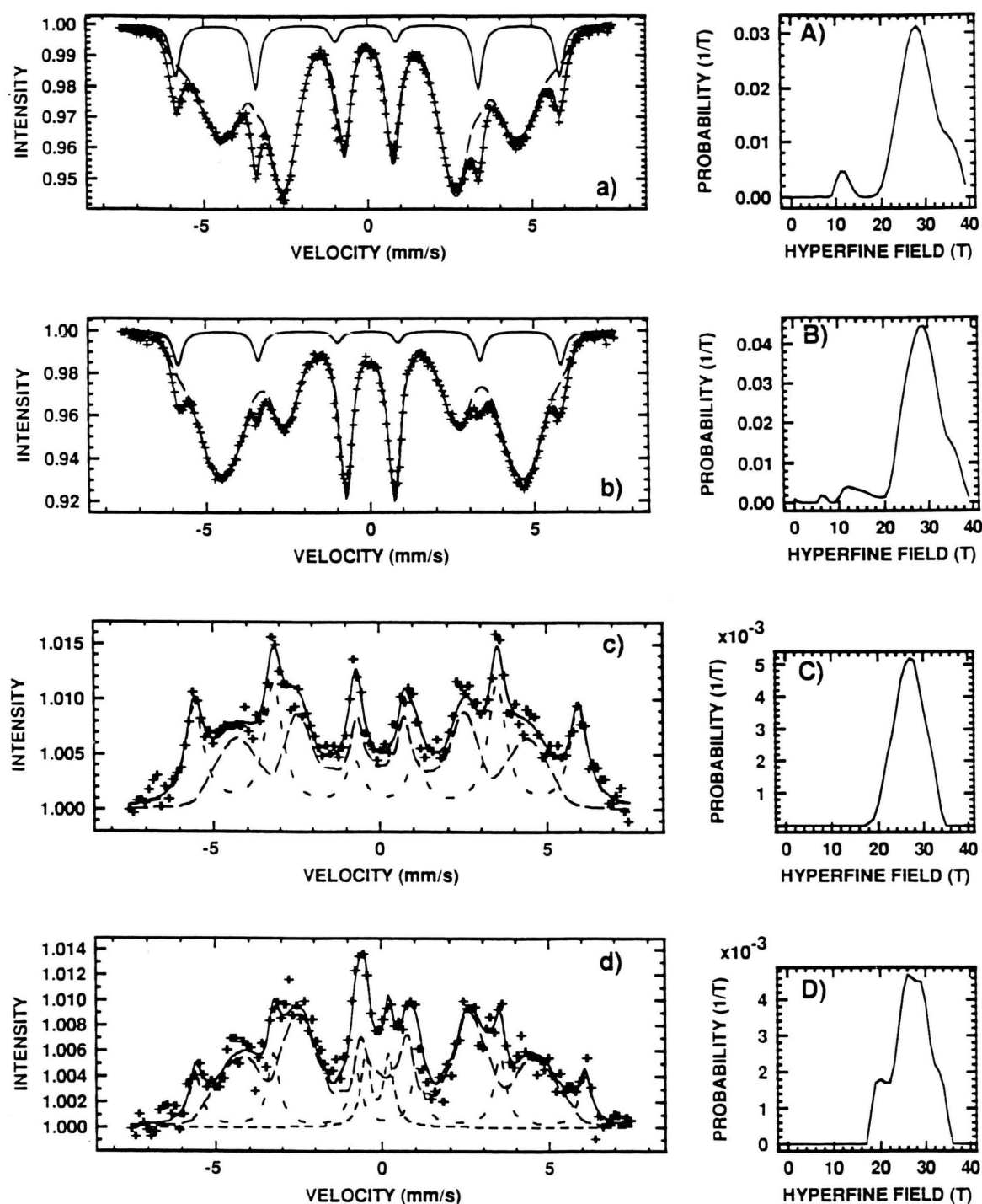


Fig. 1. Room-temperature Mössbauer spectra of the $\text{Fe}_{66}\text{Co}_{18}\text{B}_{15}\text{Si}_1$ samples, after thermal annealing at 648 K for 1 hour and subsequent pulsed-excimer-laser irradiation: (a) transmission Mössbauer spectrum of thermally-annealed sample; (b) transmission Mössbauer spectrum of thermally-annealed and excimer-laser-irradiated sample; (c) CEMS spectrum of thermally-annealed sample; (d) CEMS spectrum of thermally-annealed and excimer-laser-irradiated sample. The corresponding hyperfine magnetic field distributions extracted from the Mössbauer spectra are presented in (A)–(D).

Table 1. Hyperfine magnetic field H_{hf} , isomer shift δ (relative to α -Fe at 300 K), quadrupole splitting ΔE_Q , intensity ratio R_{21} , and relative areas corresponding to component patterns in the transmission and conversion electron Mössbauer spectra of $\text{Fe}_{66}\text{Co}_{18}\text{B}_{15}\text{Si}_1$ samples, thermally-annealed at 648 K for 1 hour and excimer laser irradiated.

Treatment of samples	Type of data	Subsp. no.	H_{hf} (kOe)	δ (mm/s)	ΔE_Q (mm/s)	R_{21}	Relative areas (%)	Assignment of phases
thermally annealed	bulk	I	362.1	0.04		1.25	11.5	α -(FeCo)
		II	279.3	0.03		0.95	88.5	amorphous
	surface	I	356.9	0.05		0.92	46.1	α -(FeCo)
		II	231.7	0.04		0.78	53.9	amorphous
thermally annealed and laser irradiated	bulk	I	360.9	0.05		0.88	7.1	α -(FeCo)
		II	278.9	0.02		0.36	92.9	amorphous
	surface	I	362.0	0.04		0.41	24.2	α -(FeCo)
		II		0.15	0.78	1.00	7.3	FeO
		III	242.1	0.04		0.99	68.5	amorphous
Errors:			± 1.5	± 0.015	± 0.02	± 0.02	± 1.0	

nealing at 648 K and subsequent pulsed-excimer-laser treatment. The hyperfine magnetic field distributions extracted from these spectra are given in Figs. 1 C and 1 D, respectively. It can be observed in Table 1 that the α -(FeCo) content of the 100 nm thick surface layer probed decreased from 46.1% in the partially-crystallized system to 24.2% in the laser-exposed specimen. As indicated by the corresponding R_{21} values, the magnetic-moment directions in the upper surface layer exhibit a preferred in-plane orientation, similar to that observed for the as-quenched ribbon. When compared to bulk measurements, this result demonstrates a different behavior of the surface magnetic texture upon irradiation, suggesting the occurrence of a distribution of magnetic-moment directions through the thickness of the foil [2]. In addition to the six-line pattern corresponding to the α -(FeCo) crystalline phase and the magnetic field distribution associated with the remaining amorphous matrix, CEMS analysis reveals the presence of a quadrupole-split doublet in the spectrum of the laser-irradiated sample, which has been assigned to nonstoichiometric iron oxides [2, 11]. Indeed, an oxidation mechanism of Fe^0 to Fe^{2+} , which initially leads to precipitation of FeO particles, can be assumed [12]. Consequently, the nature of the laser-induced phase transformation in partially-crystallized $\text{Fe}_{66}\text{Co}_{18}\text{B}_{15}\text{Si}_1$ specimens was elucidated and found to consist of partial amorphization and surface oxidation of the irradiated material. One may note that the effect of excimer-laser-induced crystallization, recently observed [2] in a $\text{Fe}_{77}\text{Cr}_2\text{B}_{16}\text{Si}_5$ amorphous alloy at high repetition rates and laser

fluences, was also shown to be accompanied by the precipitation of FeO particles on the irradiated surface.

Correspondingly, the SEM examination of the partially-crystallized $\text{Fe}_{66}\text{Co}_{18}\text{B}_{15}\text{Si}_1$ system after pulsed-excimer-laser irradiation reveals intriguing features in the region of laser-pulse incidence on the surface of the thermally-annealed alloy sample (upper left corner of the micrograph in Figure 2). The uniform aspect of the laser-irradiated area is indicative of amorphous phase formation, due to laser-induced melting and rapid solidification. This demonstrates that the laser treatment performed resulted in redissolution of most precipitate particles. The molten zones which subsequently resolidified following pulsed-laser irradiation give rise to complex internal stresses, which are responsible for the observed out-of-plane reorientation of the bulk magnetization direction. An additional morphological feature observable in the SEM micrograph of Fig. 2 is represented by the formation of droplets on the laser-irradiated surface. One may note that the single-pulse energy density employed was above the reported threshold of $\sim 2 \text{ J/cm}^2$ for the ablation of transition metals [13]. The droplet effect is attributed to laser-induced shock waves [2, 14, 15], which determine boiling of the metal surface and plasma production, due to a dramatic increase in the surface temperature and a simultaneous decrease in the metal's reflectivity. Expulsion of droplets from the laser-induced melt on the irradiated surface demonstrates an enhanced momentum transfer from plasma to target material [16], due to the recoil pressure of the breakdown plasma expansion. On these grounds, it

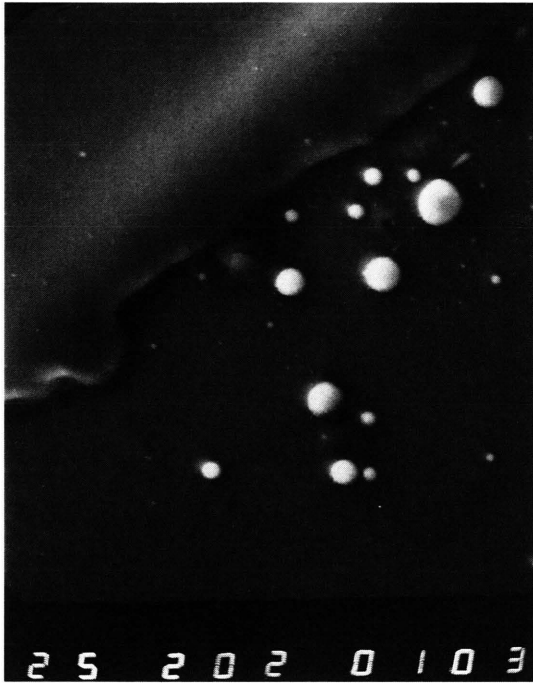


Fig. 2. SEM examination of the $\text{Fe}_{66}\text{Co}_{18}\text{B}_{15}\text{Si}_1$ sample, after thermal annealing at 648 K for 1 hour and subsequent pulsed-excimer-laser irradiation ($\lambda = 308$ nm, $\tau = 10$ ns, $\Phi_L = 5 \times 10^{18}$ photons/cm², repetition rate 1 Hz).

can be inferred that ablation pressures are high enough to change interatomic distances and cause revitrification of the laser-irradiated material.

Aiming at a complete characterization of the effects associated with the interaction of pulsed laser

radiation with Fe-Co based metallic glasses, in what follows we present investigations of the influence of excimer laser treatment on the phase composition and magnetic behavior of totally-crystallized $\text{Fe}_{66}\text{Co}_{18}\text{B}_{15}\text{Si}_1$ samples.

Figure 3a shows the room-temperature transmission Mössbauer spectrum of the $\text{Fe}_{66}\text{Co}_{18}\text{B}_{15}\text{Si}_1$ sample, after thermal annealing at 723 K for 1 hour. The spectrum was analyzed considering two six-line patterns, corresponding to the α -(FeCo) and $(\text{FeCo})_3(\text{BSi})$ crystalline phases. The relative abundance of crystalline phases (Table 2) is different for the upper 100 nm surface layer. Moreover, an additional crystalline phase, identified as $(\text{FeCo})_2(\text{BSi})$ was revealed by CEMS spectrum analysis (Figure 3c). The phase identification results obtained in the present study are in good agreement with the crystalline phase formation observed by radiofrequency annealing of $\text{Fe}_x\text{Co}_{78-x}\text{Si}_9\text{B}_{13}$ amorphous alloy [17]. The totally-crystallized $\text{Fe}_{66}\text{Co}_{18}\text{B}_{15}\text{Si}_1$ sample was further exposed to pulsed-excimer-laser irradiation ($\Phi_L = 5 \times 10^{18}$ photon/cm²) with 2 laser pulses per spot at a repetition rate of 1 Hz. The room-temperature transmission and conversion electron Mössbauer spectra of the irradiated $\text{Fe}_{66}\text{Co}_{18}\text{B}_{15}\text{Si}_1$ specimen are shown in Figs. 3b and 3d, respectively. It can be observed in Table 2 that the bulk α -(FeCo) content decreased from 66.3% in the completely-crystallized sample to 30.3% in the laser-exposed specimen. The most interesting result obtained from phase analysis of the laser-irradiated $\text{Fe}_{66}\text{Co}_{18}\text{B}_{15}\text{Si}_1$ system, however, is the absence of the $(\text{FeCo})_3(\text{BSi})$ crystalline

Table 2. Hyperfine magnetic field H_{hf} , isomer shift δ (relative to α -Fe at 300 K), quadrupole splitting ΔE_Q , intensity ratio R_{21} , and relative areas corresponding to component patterns in the transmission and conversion electron Mössbauer spectra of $\text{Fe}_{66}\text{Co}_{18}\text{B}_{15}\text{Si}_1$ samples, thermally-annealed at 723 K for 1 hour and excimer laser irradiated.

Treatment of samples	Type of data	Subsp. no.	H_{hf} (kOe)	δ (mm/s)	ΔE_Q (mm/s)	R_{21}	Relative areas (%)	Assignment of phases
thermally annealed	bulk	I	360.5	0.05		0.54	66.3	α -(FeCo)
		II	232.5	0.09		0.84	33.7	(FeCo) ₃ (BSi)
	surface	I	362.9	0.05		0.83	53.8	α -(FeCo)
		II	295.9	0.11		0.83	24.7	(FeCo) ₂ (BSi)
		III	219.9	0.08		0.83	21.5	(FeCo) ₃ (BSi)
thermally annealed and laser irradiated	bulk	I	361.8	0.06		0.35	30.3	α -(FeCo)
		II	275.0	0.04		0.41	69.7	amorphous
	surface	I	359.1	0.05		0.48	30.3	α -(FeCo)
		II		0.15	0.78	1.00	6.1	FeO
		III	208.1	0.03		0.16	63.6	amorphous
Errors:			± 1.5	± 0.015	± 0.02	± 0.02	± 1.0	

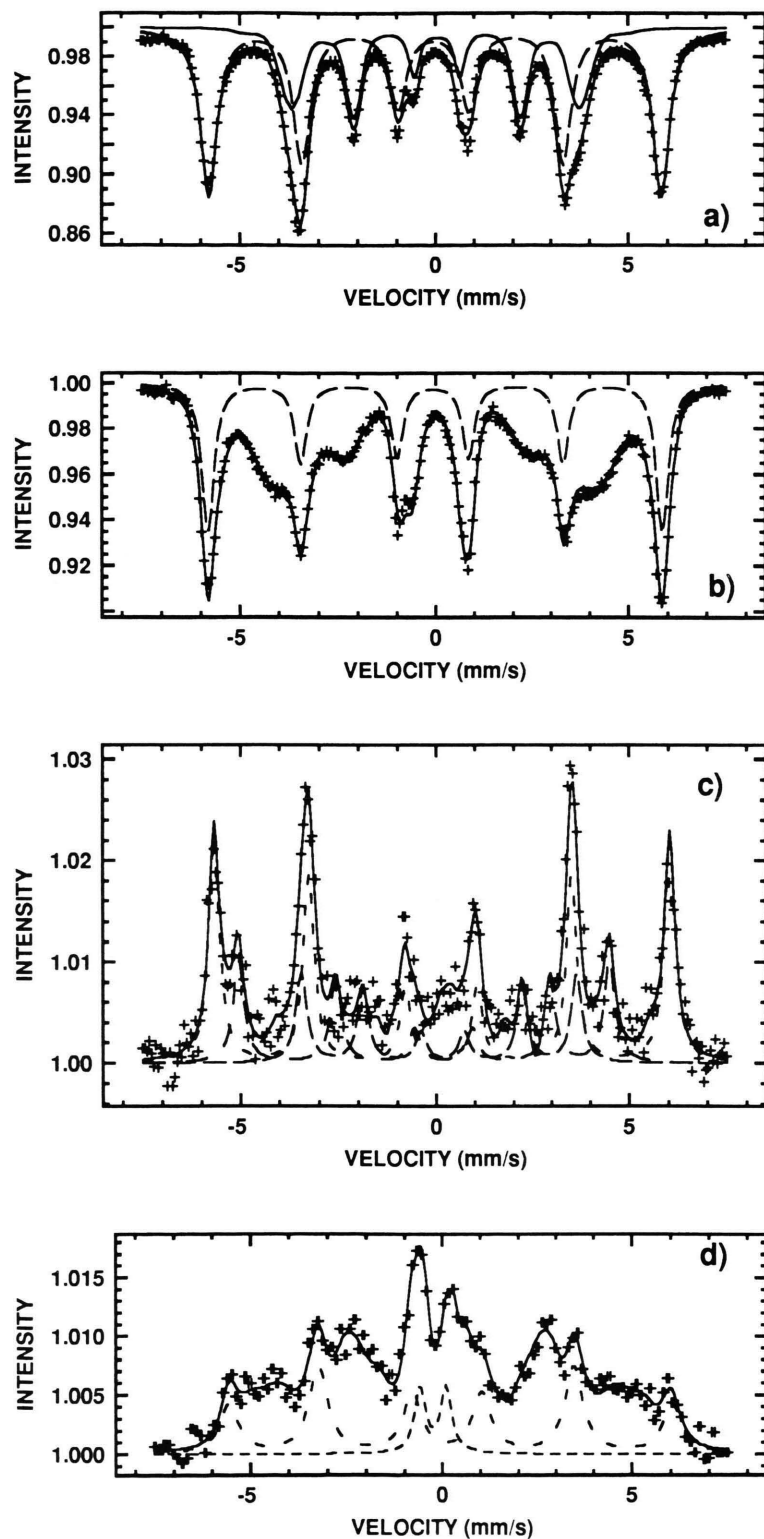


Fig. 3. Room-temperature Mössbauer spectra of the $\text{Fe}_{66}\text{Co}_{1.8}\text{B}_{1.5}\text{Si}_1$ samples, after thermal annealing at 723 K for 1 hour and subsequent pulsed-excimer-laser irradiation: (a) transmission Mössbauer spectrum of thermally-annealed sample; (b) transmission Mössbauer spectrum of thermally-annealed and excimer-laser-irradiated sample; (c) CEMS spectrum of thermally-annealed sample; (d) CEMS spectrum of thermally-annealed and excimer-laser-irradiated sample.

component, formed in the second stage of the crystallization process by thermal annealing. Instead, the balance of the composition is represented by an amorphous phase, in which a pronounced out-of-plane reorientation of the magnetic-moment directions resulted as an effect of the laser irradiation performed. Consequently, the present study shows that the effect of excimer-laser-induced amorphization in totally-crystallized $\text{Fe}_{66}\text{Co}_{18}\text{B}_{15}\text{Si}_1$ system exhibits phase selectivity with respect to the crystalline components of the ferromagnetic alloy. As in the case of partially-crystallized $\text{Fe}_{66}\text{Co}_{18}\text{B}_{15}\text{Si}_1$ system, the laser-induced amorphization was found to be accompanied by the development of an out-of-plane magnetic anisotropy.

CEMS surface analysis of the totally-crystallized, laser-irradiated $\text{Fe}_{66}\text{Co}_{18}\text{B}_{15}\text{Si}_1$ system (Fig. 3d) supports the bulk Mössbauer results: the $(\text{FeCo})_3(\text{BSi})$ and $(\text{FeCo})_2(\text{BSi})$ crystalline phases are absent, due to excimer-laser-induced amorphization, from the composition of the irradiated specimen. In the upper surface layer, the relative abundance of the stable α -(FeCo) crystalline phase, formed in the primary crystallization process of the $\text{Fe}_{66}\text{Co}_{18}\text{B}_{15}\text{Si}_1$ alloy, decreased from 53.8% in the completely-crystallized sample to 30.3% in the laser-exposed specimen. In addition to the dominant amorphous component, CEMS analysis reveals the presence of the quadrupole-split doublet corresponding to FeO particles.

Consequently, the nature of the laser-induced phase transformation in totally-crystallized $\text{Fe}_{66}\text{Co}_{18}\text{B}_{15}\text{Si}_1$ specimens is found to consist of partial amorphization and surface oxidation of the irradiated material. Excimer-laser-induced revitrification exhibits selectivity with regard to the component crystalline phases in the

annealed $\text{Fe}_{66}\text{Co}_{18}\text{B}_{15}\text{Si}_1$ system and is accompanied by laser-induced reorientation of the average bulk magnetization direction. The present results suggest that excimer laser irradiation of glassy ferromagnets promotes selective control over important structural and magnetic characteristics of the material, which has not been achieved using conventional processing methods.

Conclusions

The main results obtained in the present study can be summarized as follows:

- (i) Pulsed-excimer-laser irradiation causes revitrification of partially-crystallized $\text{Fe}_{66}\text{Co}_{18}\text{B}_{15}\text{Si}_1$ samples. The effect of excimer-laser-induced amorphization is accompanied by changes in the bulk magnetization direction.
- (ii) In totally-crystallized $\text{Fe}_{66}\text{Co}_{18}\text{B}_{15}\text{Si}_1$ specimens, laser-induced partial amorphization exhibits phase selectivity relative to the crystalline components in the alloy system. Differences between surface and bulk behavior of the magnetic texture and phase composition were observed.
- (iii) Excimer laser irradiation of metallic glasses offers the intriguing opportunity of obtaining hybrid materials with select structural and magnetic characteristics.

Acknowledgements

This work has been supported by the National Science Foundation and the Office of Naval Research.

- [1] M. Sorescu and E. T. Knobbe, *J. Mater. Res.* **8**, 3078 (1993).
- [2] M. Sorescu and E. T. Knobbe, *Phys. Rev. B* **49**, 3253 (1994).
- [3] M. Sorescu, E. T. Knobbe, D. Barb, D. Sorescu, and I. Bibicu, *Hyperfine Interact.* **92**, 1347 (1994).
- [4] M. Sorescu, E. T. Knobbe, and D. Barb, *Phys. Rev. B* **51**, 840 (1995).
- [5] M. Sorescu, E. T. Knobbe, and D. Barb, *J. Phys. Chem. Solids* **56**, 79 (1995).
- [6] M. Sorescu, J. D. Barrie, J. J. Martin, and E. T. Knobbe, *Solid State Commun.* **94**, 407 (1995).
- [7] M. Sorescu, J. D. Barrie, J. J. Martin, E. T. Knobbe, and D. Barb, *J. Mater. Sci.* **30**, 5944 (1995).
- [8] J. J. Spijkerman, *Mössbauer Effect Methodology* **7**, 85 (1971), Ed. I. J. Gruverman, Plenum, New York.
- [9] R. A. Brand, J. Lauer, and D. M. Herlach, *J. Phys. F* **13**, 675 (1983).
- [10] G. A. Stergioudis, J. Yankinthos, P. J. Rentzeperis, Z. Bojarski, and T. J. Panek, *J. Mater. Sci.* **27**, 2468 (1992).
- [11] M. Rogalski and I. Bibicu, *Mater. Lett.* **13**, 32 (1992).
- [12] W. Meisel, *J. Phys. (Paris) Colloq. Suppl.* **41**, C1–63 (1980).
- [13] J. C. S. Kools, *Pulsed Laser Deposition of Thin Films*, 456 (1994), Ed. D. B. Chrisey and G. K. Hubler, Wiley, New York.
- [14] A. P. Radlinski, A. Calka, and B. Luther-Davies, *Phys. Rev. Lett.* **57**, 3081 (1986).
- [15] C. Thomsen, H. T. Grahn, H. J. Maris, and J. Tauc, *Phys. Rev. B* **34**, 4129 (1986).
- [16] J. Hermann, C. Boulmer-Leborgne, B. Dubreuil, and I. N. Mihailescu, *J. Appl. Phys.* **74**, 3071 (1993).
- [17] M. Kopcewicz, M. El Zayat, and U. Gonser, *J. Magn. Magn. Mater.* **72**, 119 (1988).